

## CONTACT STRESSES IN CONICAL ROLLERS UNDER NORMAL AND TANGENTIAL LOADINGS

M. Wasim Akram<sup>1</sup>, A. Rayhan Md. Ali<sup>2</sup> and S. C. Chowdhury<sup>2</sup>

<sup>1</sup>Department of Ocean Engineering, Florida Atlantic University, Florida, USA

<sup>2</sup>Department of Mechanical Engineering, Bangladesh University of Engineering and Technology, Dhaka, Bangladesh

### ABSTRACT

In this paper, the stresses distributions arising from the contact between two complex geometrical bodies have been analyzed using finite element simulation software by considering two conical rollers, where two rollers have been subjected under normal compressive and tangential loading. Due to these types of loading the contact patch has been found trapezoidal shape which is in contrast with cylindrical contact, where contact patch is rectangular. The trapezoid shape of the contact area arises because the radius of curvature of either cone varies along the axial direction and contact length. So, radius of curvature is a function of vertex angle and contact length. Maximum pressure distribution and half width distribution has been found along contact length. Stresses in different directions have been analyzed and shown with different contact geometries. Maximum stresses have been found at contact surface for three normal stress components under combined loadings, and maximum shear stress has been found at some distance into the solid from contact surface. The results have been verified with analytical solutions. The finite element simulation results have been found consistent with the analytical results in predicting pressure, its distribution and stresses in contact rollers.

**Keywords:** Conical Rollers, Radius of Curvature, Finite Element Simulation, Stress Distribution.

### 1. INTRODUCTION

Loading transfer between components in engineering assemblies often causes very high localized stresses, generally called contact stresses, which lead to component failure by different forms of surface contact fatigue. Consequently, the evaluation of contact area geometries, pressure distribution, stresses is imperative to prevent premature failure such as pitting, spalling, false brinelling.

The analysis of contact stresses between simple geometries like cylindrical elements or spherical elements have attracted the attentions of many researchers. There are lots of works on these simple geometries. Heinrich Hertz[1] for the first time analyzed the contact stresses by determining the loading distribution over the contact area and provided the mathematical models for the stress field using a potential function for the case of spherical contact. He deduced that an ellipsoidal distribution of pressure would satisfy the boundary conditions of the problem for the case of spherical contact. He verified his analytical results by running a series of experiments. Hertz only considered spherical contact for his analysis. And for a long time there was no remarkable research on contact problems. Every contact problems were solved on Hertz spherical contact theory. Lundberg [2] analyzed the problem when two bodies of different geometries come in contact. He calculated the stresses for the case of a cylinder and a

spherical ball pressed on a flat plate and verified his findings by photo elastic technique. Both (Hertz and Lundberg) considered only normal loading for their analysis. But for the case of contact between two rotating elements, there is always tangential traction except pure rolling. So in that case there exist some tangential loading. Mindlin [3] investigated the stress distribution due to tangential loading when one elastic body slides over the other across the contact area for the case of cylindrical contact. Mindlin found that the stresses on the bounding curve of the contact area due to bounding curve are infinite and consequently a state of impending slipping prevails. Smith and Liu [4] studied the contact between parallel rollers in combined rolling and sliding for spherical contact only. Though there are lots of works on gear contact, cam – follower contacts and so on, but all of these were based on simple contact geometries. With advent of time more complex geometries evolved and hence researches were needed on complex geometries. Al Zain [5] analyzed the contact problem between two conical rollers only under the normal loading. Shakoor[6] also agreed with Zain's proposal while he was doing research on special cam follower contact problems. Later Litvin [7] has used Zain's proposal for his research of bevel gear. But no one did research on conical rollers for complex loading and also finite element verification.

This work was based on more complex geometries

rather than simple geometries by considering conical rollers are in contact [8] under both normal and tangential loading. The stresses due to conical rollers in contact with application of both normal and tangential loading have been solved using finite element simulation software ANSYS [9]. The results obtained from ANSYS have been verified with analytical solution. The distribution of stresses has been observed for different contact geometrical parameters and loading conditions.

## 2. ANALYTICAL SOLUTION

When two geometrically and materially identical conical rollers come into contact with each other under the application of a uniform compressive normal loading in rolling, the contact patch appears in the form of trapezoid, in contrast with two cylinders where the contact area is a rectangle.

### 2.1 Radius of Curvature

The radius of curvature of a conical roller is equal to the radius of curvature of an ellipse formed by a cut plane normal to the external surface of the conical roller. This radius of curvature varies as the cut plane moves along the contact length. Figure -1 shows two ellipses in a side view formed by sectioning conical rollers by the cut plane at  $t$ .

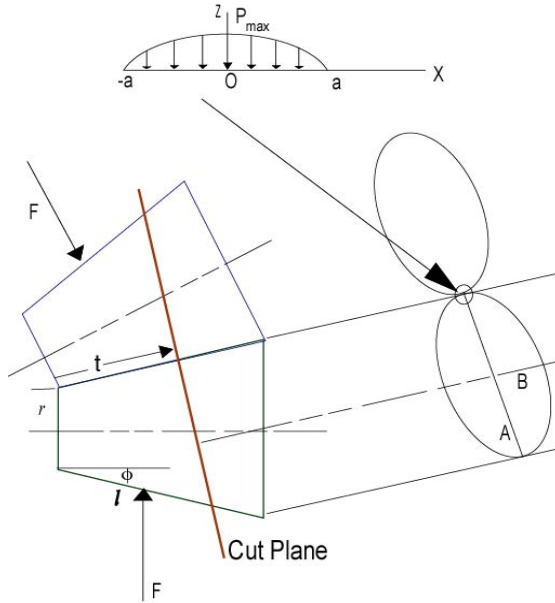


Fig 1. Two conical rollers in contact

The radius of curvature of the osculating rollers for the section at  $t$  is –

$$R_1 = R_2 = R = f(t) = \frac{B^2}{A} \quad 0 \leq t \leq l \quad (1)$$

Equation (1) is a parametric form of radius  $R$  of curvature, where all values of  $R$  along the contact length can be determined as  $t$  increases from 0 to  $l$ .  $A$  and  $B$  are the lengths of the major and minor axis respectively of the ellipses of osculating rollers 1 and 2 at  $t$ , when viewed perpendicular to the section, as shown in figure 1. The lengths of the major and minor axes, which are also

function of  $t$ , are determined by visualizing the cone in a three dimensional space. From figure 2 the length of the minor axis of each cone is –

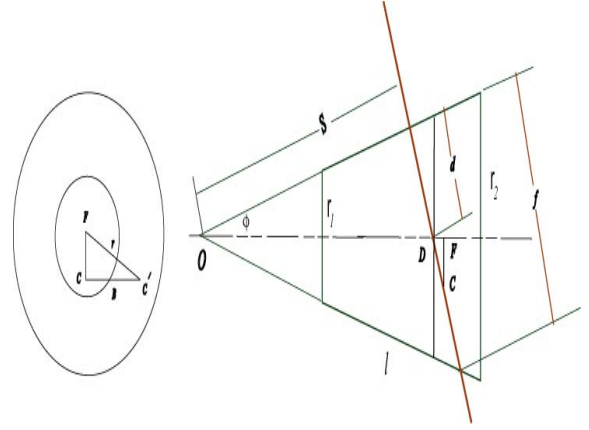


Fig 2. Front side view of conical cylinder

$$B = \sqrt{r^2 - FC^2} = \sqrt{(OD + DF)^2 \tan^2 \phi - DC^2 \cos^2 \phi}$$

$$\text{for } 0 < \phi < 45 \quad (2)$$

Where  $r$  is the radius of each cone at  $t$  and  $\phi$  is the vertex angle. The application of the above equation requires a vertex angle greater than  $0^\circ$  and less than  $45^\circ$ . At 0, the cone reduces to a line and at  $45^\circ$  the cutting plane  $t$  becomes parallel to the side  $l$ .

Putting the values of  $OD$ ,  $DF$  and  $DC$  in the above equation gives

$$B = \sqrt{\left[ \frac{S^2}{\cos^2 \phi} + \left( \frac{f-d}{2} \right)^2 \sin^2 \phi + 2 \left( \frac{S}{\cos \phi} \right) \left( \frac{f-d}{2} \right) \right] \tan^2 \phi - \left( \frac{f-d}{2} \right)^2 \cos^2 \phi}$$

$$\text{For } 0 < \phi < 45 \quad (3)$$

where  $S$  is the distance from the apex, and  $f$  is length of the section, perpendicular to the cone surface, at  $t$  projected on the  $Y-Z$  plane passing through the axis of the cone. The above equation can be written in terms of  $t$  as

$$B = K \left( \frac{r_1}{\sin \phi} + t \right) \quad 0 \leq t \leq l, \quad 0 < \phi < 45^\circ \quad (4)$$

where  $K$  is a constant which is given by

$$K = \sqrt{\left( \frac{1}{\cos^2 \phi} + H^2 \sin^2 \phi + \frac{2H}{\cos \phi} \right) \tan^2 \phi - H^2 \cos^2 \phi} \quad (5)$$

$$H = \frac{\tan(2\phi)}{2} - \tan \phi$$

The length of the major axis of each cone is –

$$A = \left( \frac{r_1}{\sin \phi} + t \right) \frac{\tan(2\phi)}{2} \quad 0 \leq t \leq l \quad 0 < \phi < 45^\circ \quad (6)$$

Putting the values of equations (4) and (6) in equation (1) gives –

$$R = \frac{2K^2}{\tan(2\phi)} \left( \frac{r_1}{\sin \phi} + t \right) \quad 0 \leq t \leq l \quad 0 < \phi < 45^\circ \quad (7)$$

The conical roller geometric constant  $b$  that depends only on the radii of curvature of two cones, at  $t$  is –

$$b = \frac{1}{2} \left( \frac{1}{R} + \frac{1}{R} \right) = \frac{1}{R} \quad 0 \leq t \leq l \quad (8)$$

It may be noted that like  $b$ , has a unique value for each value of  $t$  as long as long radius of curvature is not infinite or undefined.

## 2.2 Stress Distribution

Plane strain conditions have been assumed. The other two stresses ( $\sigma_x$  and  $\sigma_z$ ) have been determined first by considering point loading distribution for normal and tangential loading and hence integrating over the deformed area i.e. contact patch. Von misses shear stress ( $\tau_{xz}$ ) has been analyzed using normal stresses. Following equations were used for stress distribution-

$$\sigma_x = -\frac{2z}{\pi} \int_{-a}^a \frac{p(s)(x-s)^2 ds}{\{(x-s)^2 + z^2\}^2} - \frac{2z}{\pi} \int_{-a}^a \frac{q(s)(x-s)^3 ds}{\{(x-s)^2 + z^2\}^2} \quad (9)$$

$$\sigma_z = -\frac{2z^3}{\pi} \int_{-a}^a \frac{p(s)ds}{\{(x-s)^2 + z^2\}^3} - \frac{2z^2}{\pi} \int_{-a}^a \frac{q(s)(x-s) ds}{\{(x-s)^2 + z^2\}^2}$$

$$\sigma_y = \nu(\sigma_x + \sigma_z) \quad (10)$$

$$\tau_{xz} = \left| \frac{\sigma_x - \sigma_z}{2} \right| \quad (11)$$

## 2.3 Other Equations

For tangential loading –

$$q(x) = \pm \mu p(x) \quad (12)$$

Half width-

$$a = \sqrt{\frac{2(m_1 + m_2)F}{\pi bl}} \quad (13)$$

It is noted that half width does not vary with tangential loading if the material properties of two mating bodies are identical.

Pressure Distribution and Maximum Pressure

$$p(x) = P \max \sqrt{1 - \frac{x^2}{a^2}} \quad (14)$$

$$P_{\max} = 2*F / \pi a l \quad (15)$$

## 3. FINITE ELEMENT SIMULATION

In order to analyze conical rollers in finite element model, a geometrical model was created using Solid Works software. The length of the two rollers was 20 mm and vertex angle was 5 degree. The radiuses at the tip were 5 mm for both rollers. Then the geometrical model was transferred to ANSYS finite element software. After that, geometrical modeling was completed by creating surfaces using the loft method. In the meshing process, tetrahedral 10-Node element (SOLID 187) elements were employed to increase accuracy of the modeling. Materials have been used steel with  $E=209$  GPa and poisson's ratio 0.3 As in case of contact problems stress are concentrated close to contact region. So, fine mesh is required in the contact region. To do so, first all the geometrical models have been meshed freely. Then the contact surface has been mapped mesh to finer the meshing

Convergence criteria should be considered to evaluate

the results. Convergence analysis is performed on a metallic model of the conical rollers. By improving mesh density step-by-step a suitable number of elements is obtained. The stabilization of deformation and Von-Misses equivalent stress at a location far from the applied loadings are the criteria of convergence. The depiction of the FE model is shown in figure. 3. To give uniform compressive loading an almost zero thickness plate has been used.

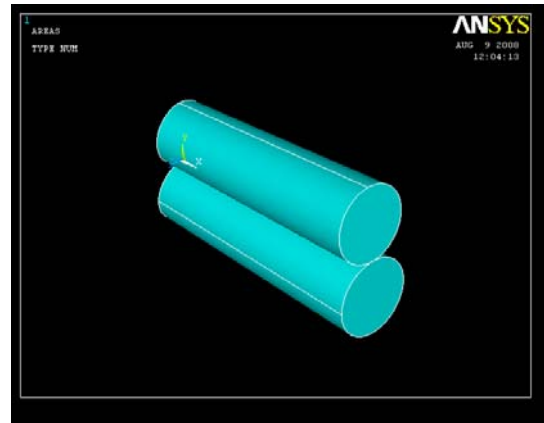


Fig 3. Finite element model

## 4. RESULTS AND DISCUSSION

In case of conical rollers in contact, the contact area is in form of trapezoid. So half width is not constant like cylindrical contacts. Though the half width is axis symmetric along line of contact but it varies along the length of the conical roller which has been shown in the figure 4. From the graph it has been observed that at the tip of conical rollers, half width has minimum dimension and it increases with the increase of length of the rollers.

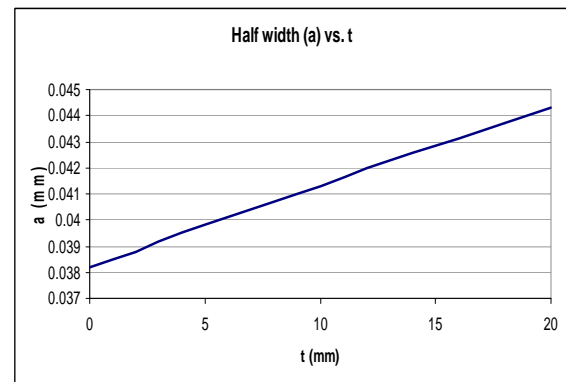


Fig 4. Half width distribution

As the maximum pressure under contact region depends on the deformed shape of the rollers, so maximum pressure has been found varying with the length of the conical rollers. At the tip of the conical rollers, the half-width is the minimum, so maximum pressure has been found largest at the tip as  $P_{\max}$  inversely proportional to half-width. The variation has been shown in the figure 5.

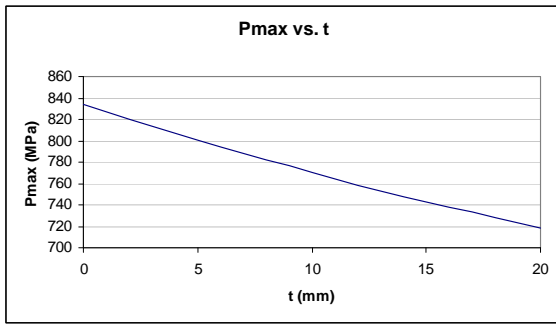


Fig 5. Maximum pressure distribution

Stress distribution for X axis ( $\sigma_x$ ) in case of normal loading has a maximum stress ratio i.e.  $\sigma_x / P_{max}$  is -1. It means that stress is compressive and maximum stress has a value same as maximum pressure. The maximum stress has been found at contact surface i.e.  $z/a=0$  and at  $x/a = 0$  i.e. at line of symmetry. For the case of tangential loading, the distribution is linear. In leading edge i.e. where rolling starts, the stress type is compressive and in trailing edge its type is tensile. The maximum stress ratio occurs at contact surface i.e.  $z/a = 0$  and a value of 0.6. In leading edge it has been found compressive at  $x/a=1$  i.e. where contact begins. In trailing edge it has been found tensile at  $x/a= -1$  i.e. where contact ends. For combined loading, the maximum stress has been found at contact surface i.e.  $z/a=0$  and it has been found at  $x/a=0.5$  distance towards the leading edge with a value of -1.167. So in case of combined loading stress component in X direction has a value 16.7% higher than that for normal loading and has been found 50% shifted towards the leading edge from symmetry. The stresses distributions for different loading have been shown from figure 6 to 8.

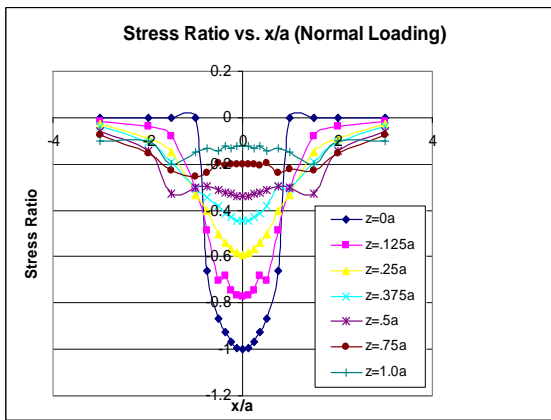


Fig 6. Distribution of  $\sigma_x$  under normal loading

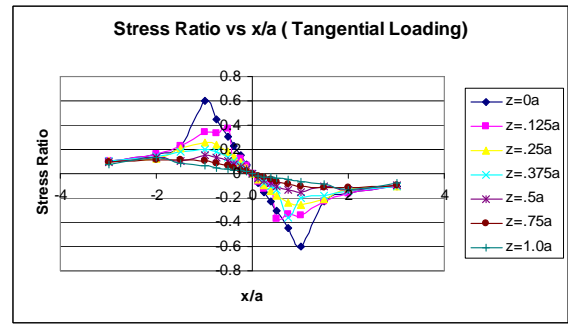


Fig 7. Distribution of  $\sigma_x$  under tangential loading

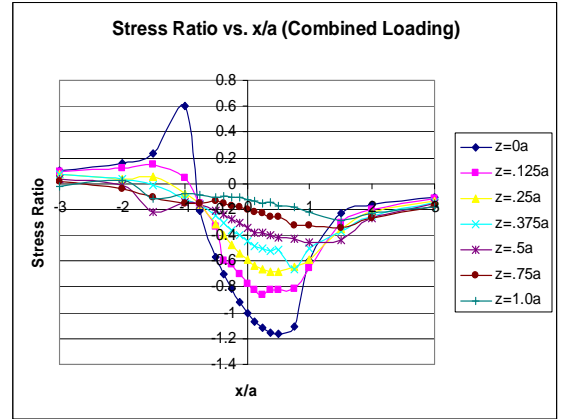


Fig 8. Distribution of  $\sigma_x$  under combined loading

As the maximum contact pressure is higher at the tip of the conical roller, so stress will be high at the tip. It decreases in value with the increases the length from the tip. In the figure 9 the stress distribution in X axis (at surface i.e.  $z/a=0$ ) for combined loading has been shown

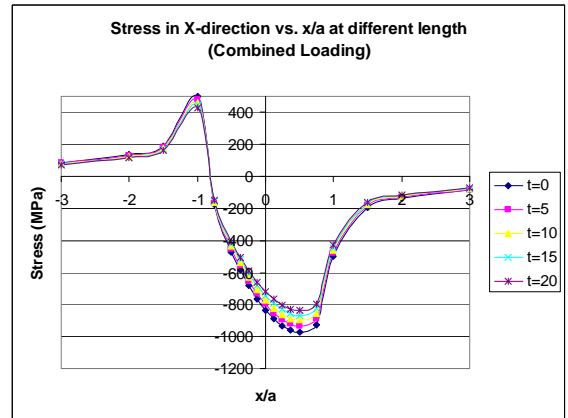


Fig 9. Distribution  $\sigma_x$  along contact length

Stress distribution in Z axis i.e. axis directed to solid vs.  $x/a$  shows that there is same distribution as pressure distribution for normal loading. The maximum stress ratio that is stress to maximum pressure has been found at  $x/a=0$  and at the surface. With increasing of the distance from the surface it decreases. The maximum value of

stress ratio is -1 that is exactly same what the value for maximum normal pressure.

The stress distribution (for tangential loading) vs.  $x/a$  shows linear relation. The stress ratio has very negligible value. It means by applying tangential loading in X direction, stress components in Z axis don't vary so much. So, for combined loading the stress distribution has shown same like for normal distribution. The stress distributions in Z axis for different loadings have been shown from figure 10 to 12.

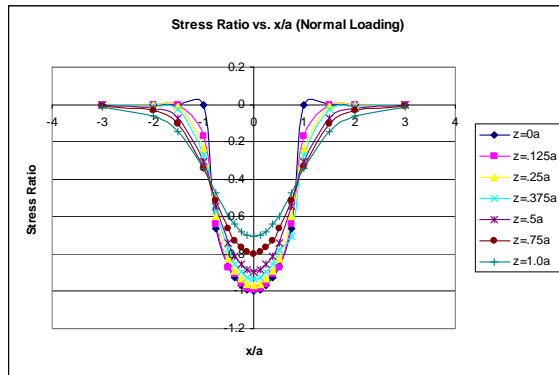


Fig 10. Distribution of  $\sigma_z$  for normal loading

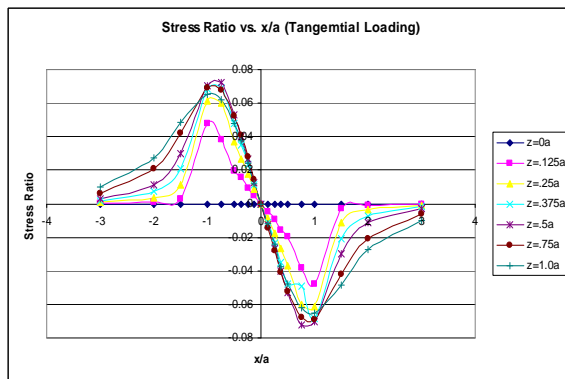


Fig 11. Distribution of  $\sigma_z$  for tangential loading

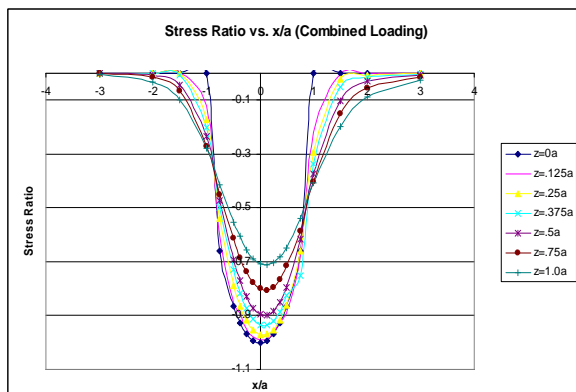


Fig 12. Distribution of  $\sigma_z$  for combined loading

Like the stress distribution in X axis, stress in Z axis also varies with varying distance from tip. At the tip i.e.

at  $t=0$ , the stress is maximum and its value decreases with increasing the distance from tip. The variation of stress along the contact length has been shown in figure 13.

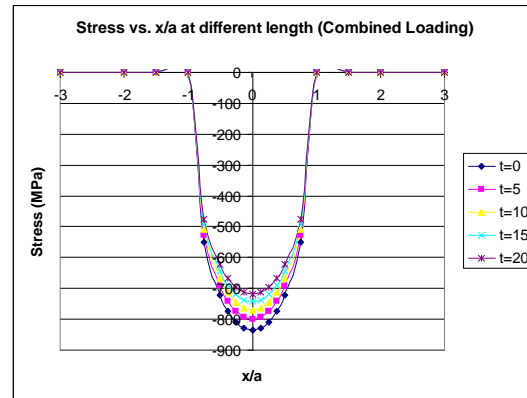


Fig 13. Distribution  $\sigma_z$  along contact length

From the distribution of stress in Y axis, we have seen that the distribution is as like as that for X axis, i.e. maximum value has been found some value tilted towards leading edge. But value of stress ratio is of 0.60 which is lower than other two components. So this stress component does not have significant role for contact stresses. The location where maximum stress has been found is at contact surface ( $z=0$ ) and at a distance ( $x/a=0.5$ ) from line of symmetry. The stress distribution has been shown in figure 14.

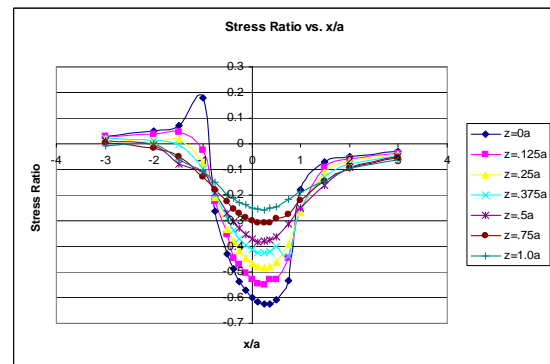


Fig 14. Distribution of  $\sigma_y$  for combined loading

From Von Mises stress distribution along  $x/a$  it has been found that maximum value for shear stress has been found that for  $z/a=0.34$  at it has been found at  $x/a=0$  with a stress ratio of 0.4. At surface  $z=0$  the value is not as high as that for  $z/a=0.30$ , though all other stress components are high at surface. The shear stress also varies with contact length. The distribution of shear stress with the variation of  $x/a$  and  $z/a$  as well contact length have been shown from figure 15 to 18.

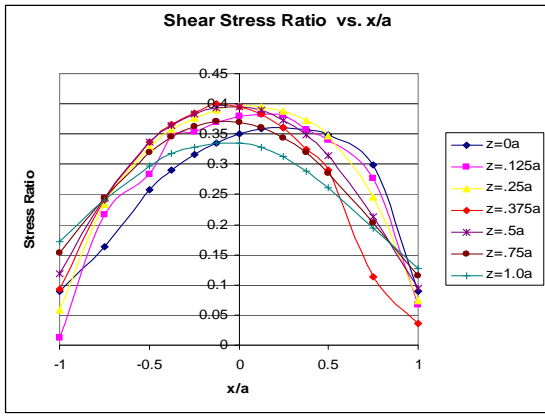


Fig 15. Distribution of shear stress along  $x/a$  (combined loading)

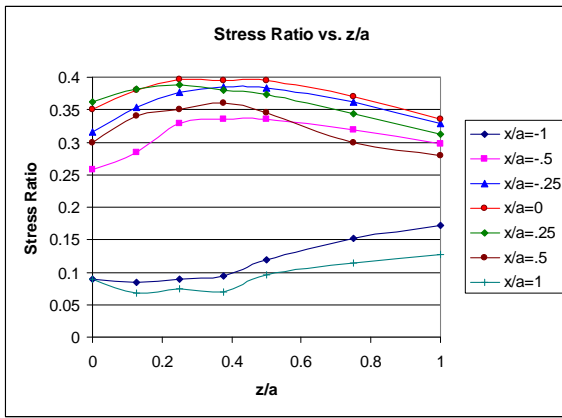


Fig 16. Distribution of shear stress along  $z/a$  (combined loading)

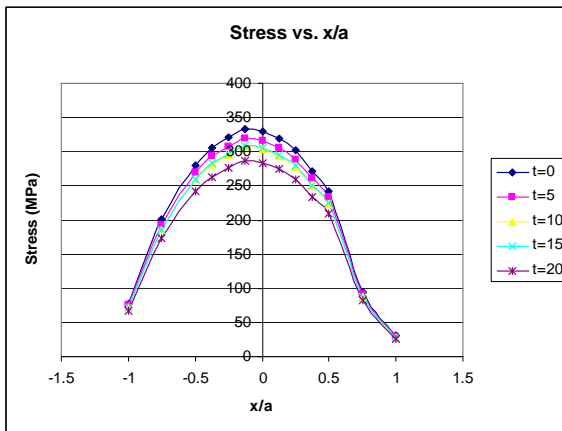


Fig 17. Distribution shear stress along contact length and  $x/a$

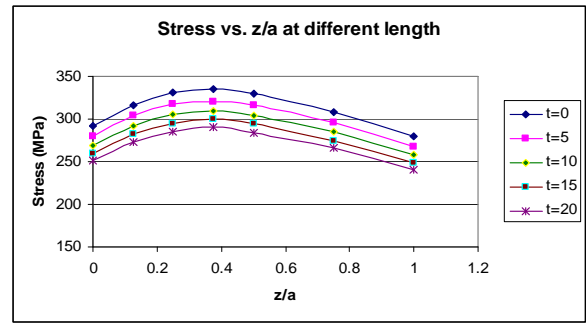


Fig 18. Distribution Shear Stress along contact length and  $z/a$

The results those have been obtained from ANSYS are very close to analytical solutions. Stress components in each direction are almost same with that of analytical results which have been solved by integration. To compare results only steel material has been considered with same loading conditions. The overall geometry and contact geometries were identical. The comparisons of the results have been shown from figure 19 to 21.

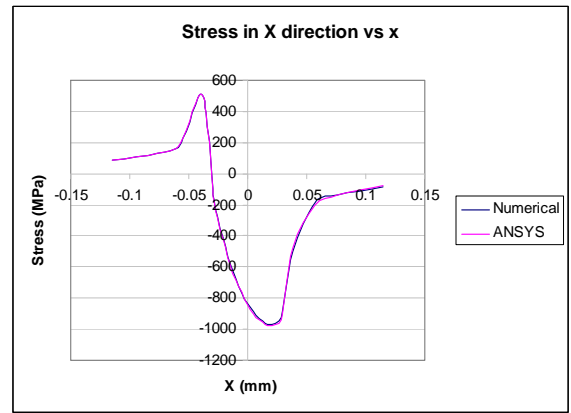


Fig 19. Comparison of  $\sigma_x$  with analytical solution

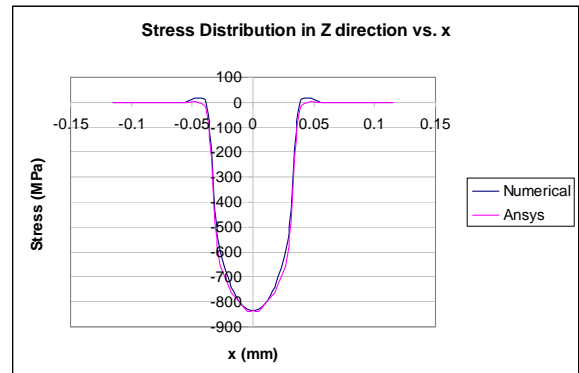


Fig 20. Comparison of  $\sigma_z$  with analytical solution



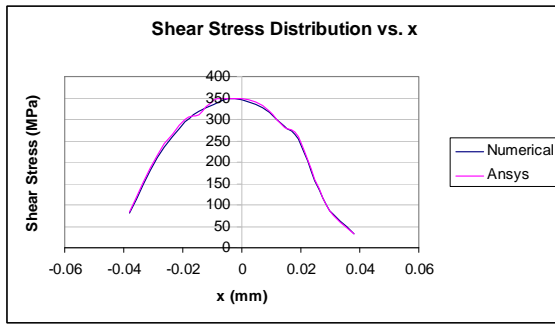


Fig 21. Comparison of shear stress with analytical solution

## 5. CONCLUSION

For simple geometries like sphere to sphere contact, cylinder to cylinder contact or cylinder to plane contact, the contact area or deformed area is either circular or rectangular based on type of contacts. But for conical rollers are in contact, the deformed area is trapezoid so half width varies with distance (from smaller end). In case of combined loading stress component in X direction has a value 16.7% higher than for normal loading and has been found 50% shifted towards the leading edge from symmetry.  $\sigma_x$  varies along the contact length. With increasing of the distance from the apex of the roller  $\sigma_x$  decreases. The variation of stress between apex and larger end of the conical roller is 13.8% i.e. at the apex of the cone the stress is 13.8% higher than that at the large end.

The maximum value of stress ratio in Z direction for the case of tangential loading is .072 i.e. very negligible in compare with normal loading which is -1. So, for combined loading the distribution is almost like stress distribution for normal loading. In case of combined loading the stress ratio is -1 and it has been found as like as normal distribution i.e. at contact surface and in the line of symmetry of pressure distribution.

For the case of contact problems, the main cause of the initiation and propagation of crack or cracks is the maximum value of shear stress. In this present work to predict maximum shear stress Von Mises Maximum Shear Stress principle has been used. The maximum value as well as location of that peak value is important. From this work, for the case of combined loading we have found that the peak value of shear stress ratio i.e. ratio of maximum shear stress and maximum pressure is 0.39 which is 7.6% higher than that for only normal loading. The location of the maximum shear stress has been found at  $x/a=0$  i.e. the line of symmetry and at  $z/a=0.30$ . So from this two works it can be found that for combined loading the location of the maximum shear stress is 20% less deep from contact surface. The results obtained from ANSYS have been found consistent with those analytical results.

## 6. REFERENCES

1. Hertz, H. Gesammelte Werke, Band I, 1895 (Basth, Leipzig) (English transl. Hertz J,H Miscellaneous papers, 1896 (Macmillan, London)

2. Lunderberg, G. Elastiche Beruehrung Zweier Halbraeume Forsch. Geb Ingenieurwesens A, 1936, 10, 201-211
3. Mindlin, F. M. Hertz Contact Problem For Elastic Anisotropic Halfspace with Initial Stress, Plenum Publishing Corporation, 1990, 126-132
4. Smith, J.O. and Liu, C.K. , Stresses due to tangential and normal loadings on an elastic solid with application to some contact stress problems. Trans. ASME J. Appl. Mechanics, 1953, 75, 157-166
5. Al-Zain, H.O. Contact stresses in conical shaped rollers. Masters thesis, Department of Mechanical Engineering, Iowa State University, 2004.
6. Ali M, Shakoor M, Fluggrad D and Qamhiyah A. Cam optimization based on a fatigue life model. In proceedings of ASME 2006 International Design Engineering Technical Conferences and Computer and Information in Engineering Conference, Philadelphia, Pennsylvania, USA, 2006, pp 1- 8 (American Society of Mechanical Engineers, Newyork).
7. Litvin, L. E. Fuentes A. and Hayasaka, K. Design manufacture, stress analysis and experimental test of low noise high endurance bevel gears. Mechanism Mach Theory, 2006 41(1), 83 -118
8. Johnson, K. L. Contact Mechanics, 1985 (Cambridge University Press)
9. ANSYS user's manual, Version 10.0 , 2007

## 7. NOMENCLATURE

Symbol	Meaning	Unit
$\sigma_x$	Stress in X direction (Along Contact)	(MPa)
$\sigma_z$	Stress in Z direction ( Into the solid)	(MPa)
$\sigma_y$	Stress in Y direction (Along the length of the roller)	(MPa)
R	Radius of curvature	(mm)
t	Distance from tip of the rollers	(cm)
l	Length of the roller	(cm)
$\phi$	Vertex Angle	( $^{\circ}$ )
a	Half Width	(mm)
P(x)	Normal Pressure Distribution	(MPa)
$P_{max}$	Maximum Pressure	(MPa)
q(x)	Pressure Due to Tangential Loading	(MPa)
S	Cut plane distance	(mm)
s	Integrating variable	(-)
E	Young's Modulus	(GPa)
$\nu$	Poisson's Ratio	(-)
$\mu$	Kinetic Friction between two rotating rollers	(-)
F	Applied Compressive Loading	(N)
r	Radius at tip of the rollers	(mm)

## 8. MAILING ADDRESS

Mohammad Wasim Akram  
 Department of Ocean Engineering ,  
 Florida Atlantic University, Florida, USA